Layer-Specific Analysis of Orientation Dependence for SSFP and EPI BOLD Signals at 9T

Kaylen Richardson*

Magnetic Resonance Center, Department of High-Field Magnetic Resonance, Max Planck Institute for Biological Cybernetics, Tübingen, Germany.

* kaylen.richardson@tuebingen.mpg.de

Abstract: The dependence of the BOLD effect as measured by Echo Planar Imaging (EPI) sequences and balanced Steady State Free Precession (bSSFP) sequences on the orientation of the cortical vasculature to the main magnetic field B_0 is examined in this study at 9.4 Tesla. The BOLD effect is generated in one volunteer subject using a breath-hold experiment, and analyzed for a relationship with the orientation of the cortex to B_0 (and therefore cortical vasculature) within five segmented cortical layers.

Zusammenfassung: Die Abhängigkeit des BOLD-Effekts von der Orientierung kortikaler Blutgefäße in Richtung das Hauptmagnetfeldes B_0 wurde in dieser Studie erforscht. In einem 9,4 Tesla Magnet wurden Probanden im Echo Planar Imaging (EPI) und balanced Steady State Free Precession (bSSFP) gescannt. Der BOLD-Effekt wurde durch ein Atem-anhalte Experiment provoziert. Die Beziehung zwischen diesem Effekt und der Orientierung des Cortex in Richtung B_0 wurde innerhalb fünf kortikaler Schichten analysiert.

Motivation

The aim of this Master's thesis is to investigate the dependence of the Blood Oxygenation Level Dependent (BOLD) effect measured with two difference fMRI pulse sequences (Echo Planar Imaging (EPI) and balanced Stead-State Free Precession (bSSFP)) on the orientation of the cortical surface and therefore cortical vasculature to the main magnetic field, B_0. This is performed through the acquisition of fMRI images using both sequences during a breath-hold hypercapnia experiment, and analyzing the correlation between the magnitude of ΔBOLD and the magnitude of cortical surface normal vector component in the direction of B_0. The expectation from theory and previous studies is that orientation dependence in the EPI sequence is a result of extravascular phase accumulation due to static field variations resulting from susceptibility differences between the deoxygenated blood in the vessel and the surrounding tissue water, and follows a shape agreeing with $\cos^2(\theta_z)$ [1]. The bSSFP sequence is sensitive to the intravascular frequency shift, which is dependent on the orientation to the main magnetic field according to Equation 1 [2]. This orientation dependence mechanism in the context of changes in the measured BOLD effect has not yet been experimentally investigated.

Eq 1:

$$\Delta\omega_{in} = 2\pi\Delta\chi_o(1-Y)\omega_o(cos^2\theta - \frac{1}{3})$$

Materials and Methods

Thirteen participants (5 male, mean age 26, age range 19-36) voluntarily took part a breath-hold behavioural study, which entailed performing a breath-hold task outside of the scanner while measuring head motion with a gyroscope. One participant (female, age 26) was then chosen based on her minimal head movement in the behavioural study to further participate in the functional imaging breath-hold experiment at a 9.4 T MR Scanner (Siemens, Erlangen, Germany).

A single run of the breath-hold paradigm consisted of three 30-second breath-holding periods, separated by 40 seconds of paced breathing (cued at a rate of 0.17 Hz). Paced breathing baseline images were acquired for 25 seconds at the beginning and at the end of each functional run, resulting in a duration of less than five minutes per run.

Images were acquired using both EPI (TR 1.26 seconds, TE 22 ms, nominal FA 70°, 220 volumes per experiment) and bSSFP (TR 2.532 seconds, nominal FA 12°, bandwidth 880 Hz/Px, acquisition of 110 volumes per experiment) sequences. The subject performed two runs for each imaging sequence. In addition to the functional images, full-brain MP2RAGE (voxel size 0.6 mm isotropic, TR 6 seconds, TE 3 seconds, inversion time 800 ms, FA 5°) and AFI (voxel size 3.3 mm isotropic, TR 20 ms, TE 2.6 ms, FA 50°) images were acquired for gray-matter segmentation and cortical layer construction.

Using house-made MATLAB scripts, a quantitative T1 map (qT1) and second inversion image (GRE2) were calculated from the MP2RAGE and AFI (MATLAB 2014b, The MathWorks, Inc., Natick, Massachusetts, United States).

The specific preprocessing protocol of the functional images tailored to each individual imaging sequence. In common between the preprocessing of the bSSFP and EPI images was the removal of baseline drift using a High Pass Filter with a cutoff time of 100 seconds for both image types, and some form of motion correction. Motion correction for the EPI images was performed with house-made MATLAB scripts and sequence-specific estimated motion parameters. Motion correction for the bSSFP images was performed using the LIPSIA "vmovcorrection" function from the LIPSIA command line tool [3]. Slice timing correction was determined to be unnecessary from visual inspection of the EPI slices, and the acquisition of the bSSFP images is performed on a per-volume basis, ruling slice timing correction for bSSFP also unnecessary. In addition to motion correction and High Pass Filtering, distortion correction was also applied to the EPI images using further house-made MATLAB scripts and a Point Spread Function (PSF) reference scan acquired using the EPI sequence.

Image analysis was performed in anatomical space. Functional EPI images were resampled to the anatomical space and coregistered to the Gradient Echo reference image of the PSF EPI scan, which was itself coregistered to the qT1 image. By concatenating these two transformations, the EPI images could be brought into anatomical space. The bSSFP images were coregistered directly with the qT1 image. All coregistration was performed using FSL's FLIRT command line tool (the Analysis Group, FMRIB, Oxford, UK).

The gray-matter segmentation and construction of cortical layers were both performed with the software MIPAV (Medical Image Processing, Analysis and Visualization; NIH, Bethesda, USA – http://mipav.cit.nih.gov) using the java pipeline plugin JIST (Java Image Science Toolkit, developed by Bogovic et al. in 2010: http://www.nitrc.org/projects/jist).

The segmented cortex was divided into five layers, in order to investigate orientation dependence on a layer-specific level. The orientation to B_0 was calculated at each voxel contained within the layers within the JIST pipeline, by calculating a surface normal at the location of the voxel. The magnitude of the component of the surface normal in the direction of B_0 is then referred to as "dz." The magnitude of breath-hold related changes in BOLD signal was calculated for each voxel contained within the layers by fitting a General Linear Model (GLM) including a 2^{nd} order Fourier Basis set to the voxel time course, which has been shown to be an appropriate model for breath-hold experiments by previous authors [5-7]. Voxels were considered "active" if the calculated coefficient of determination between the time series and the model was greater than 0.4. The magnitude of the change in BOLD was then calculated for active voxels as the amplitude of the fit model, which was then normalized the average BOLD signal of the baseline and expressed in (%).

This allowed for the calculation of a two-dimensional histogram comparing the degree of alignment to B_0 to the magnitude of the breath-hold BOLD effect for all voxels of a layer, producing a layer-specific Pearson correlation coefficient related to orientation dependence. In order to further visualize the relationship between ΔBOLD and orientation to B_0, the values for dz were also binned in increments of 0.1 and ΔBOLD averaged within each bin, to create a direct plot of ΔBOLD vs. dz.

Results

The five cortical layers constructed in JIST/MIPAV are shown in Figure 1. Layer 1 is the innermost layer, Layer 3 is the central layer, and Layer 5 is the outermost layer, including the pial surface.

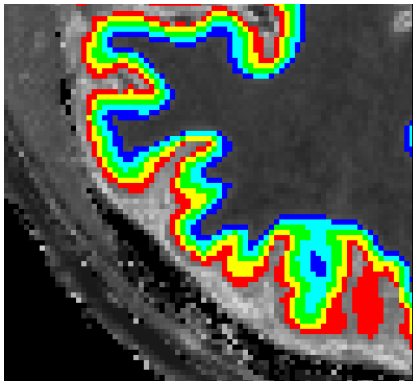

Fig. 1: Five layers constructed within the cortex of a human volunteer using the JIST pipeline environment of the software MIPAV.

The fitting of the GLM to the voxel time series resulted in 39,092 active voxels in bSSFP run 1, and 62,475 active voxels in EPI run 1. The highest percentage of active voxels was located in Layer 5, and lowest percentage in Layer 1, for both EPI and bSSFP runs. For all active voxels contained within gray-matter, the average ΔBOLD (normalized to the baseline) was found to be 4.84% (+/- 15.94) and 4.78% (+/- 61.71) for bSSFP run 1 and run 2, respectively. It was found to be 6.81% (+/-

5.34) and 6.07% (+/- 16.87) for EPI run 1 and run 2, respectively.

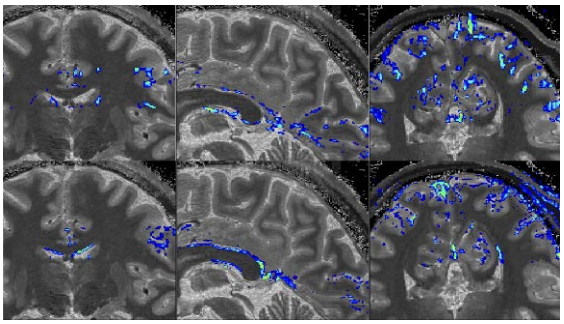

Fig. 2: Activation map for EPI run 1 (top) and bSSFP run 1 (bottom); intensity corresponds to coefficient of determination with the activation model, with applied threshold of 0.4.

Examples of Pearson correlation coefficients calculated from two-dimensional histograms for each layer are shown in Table 1. The graphs resulting from the binning of dz values in increments of 0.1 and averaging ΔBOLD over each bin are shown in Figures 3 and 4.

Tab. 1: Pearson correlation coefficient calculated between ΔBOLD and dz for all voxels in each cortical layer

	Pearson Correlation Coeff.		
Layer:	*1*	*3*	*5*
bSSFP Run 1	0.3	0.32	0.06
Run 2	0.12	0.23	0.002*
EPI Run 1	-0.016*	-0.031	0.013*
Run 2	-0.035	-0.004*	0.029*

* Pearson correlation was calculated with a p-value greater than 0.05: non-statistically significant; all other correlations statistically significant with p < 0.05

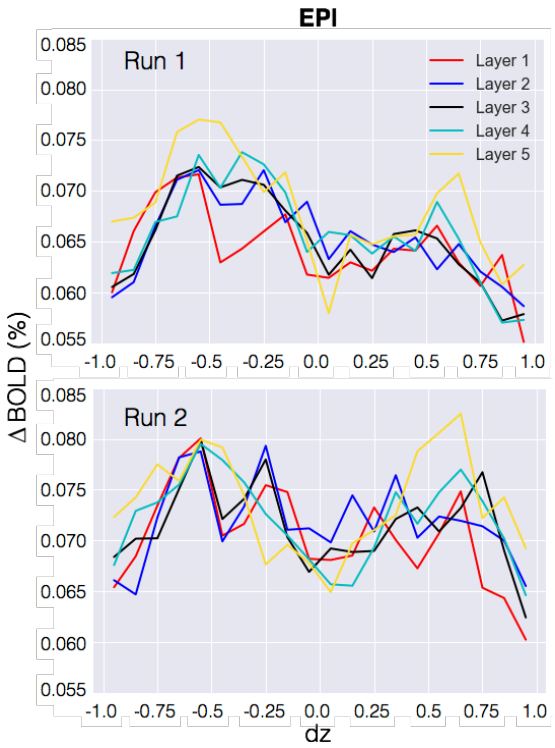

Fig. 3: Binned graphs of ΔBOLD vs. dz for both functional runs imaged using the EPI sequence.

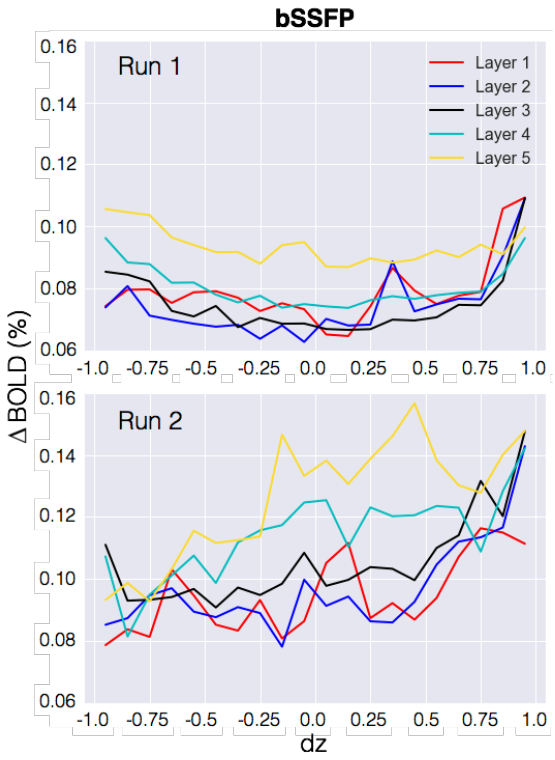

Fig. 4: Binned graphs of ΔBOLD vs. dz for both functional runs imaged using the bSSFP sequence.

Discussion

The behavioural study performed before the functional imaging study proved to be a useful measure of paradigm feasibility, and potential paradigm-related head motion. Based on the ability of the subject to consistently perform every breath-hold to the full duration, with minimal measured head motion, it was possible to select a subject who was both comfortable performing the task, and capable of performing it with a small enough range of head motion that the EPI motion correction was able to remove it completely. Unfortunately, motion correction could not be applied to the bSSFP images in the same way, leading to a less effective motion correction and some remaining paradigm-related motion in this case. The lack of effectiveness of the bSSFP motion correction is likely in part due to the lack on contrast between gray matter and white matter, which hinders the coregistration process between slices. However, from observation of the estimated motion parameters, it seems that the greatest issue with the motion correction was that the correction algorithm mistook the large signal changes due to the breath-hold for motion, and over-corrected for them. This resulted in an over-estimation of rotation (ten-times greater than the estimated rotation for EPI).

The paradigm-related motion left in the bSSFP pre-processed images resulted in activated voxels around the borders of the ventricles and in the skull, as can be seen in Figure 21. While the activation outside of the cortex is not particularly problematic for the analysis, because statistics were only performed on active voxels contained within the constructed gray matter layers, it is also an indicator that some changes within the cortex could also be related to the poor motion correction instead of the breath-hold. Therefore, more options need to be explored for motion correction of the bSSFP images.

Another area of pre-processing that requires improvement in order for the analysis pipeline for EPI images to produce reliable and accurate statistics is the coregistration of EPI images to anatomical space. In this study, the coregistration was performed in a three-step process: first, the EPI images were averaged over the repeated volumes in the run, in order to create an average 3D volume. The mean 3D volume was then coregistered to the whole-brain gradient echo PSF reference scan. The PSF reference scan was then coregistered to the qT1 image, and this transform was applied to the mean EPI volume in PSF reference space. While the transformation from PSF reference space to qT1 space was accurate, the transformation from mean EPI space to PSF reference space resulted in an offset in the order of millimeters.

The imperfect coregistration of the EPI functional data to the layers is likely the reason that few of the Pearson correlation coefficients calculated within the layers for percent change BOLD vs. dz were associated with p-values of less than 0.05 (three in run 1, one in run 2). Of the correlation coefficients that were significant, all were negative. This is in stark contrast to the correlation coefficients of the bSSFP data, for which all coefficients were positive.

The sign of the correlation can be related to vessel sensitivity: a negative correlation coefficient means that low dz (close to 0, i.e. θ_z = 90°) results in a high percent change in BOLD. This would make sense if the sequence were sensitive to the smaller penetrating vessels (such as bSSFP), which when θ_z = 90°, are oriented approximately perpendicular to B_0. As the change in BOLD should be at its greatest when vessels are aligned perpendicular to B_0, the signal for dz = 0 should be higher than for dz = 1.0. Contrarily, due to the sensitivity of the EPI sequences to the pial vessels, which are orientated perpendicular to B_0 when dz = -1.0 and 1.0, the signal change should be high at dz = 1.0 and low and dz = 0, corresponding to a positive correlation coefficient. However, in the results of this experiment, the signs of the correlation coefficients were opposite to expectation for both EPI and bSSFP.

Observing the binned orientation graphs of the functional imaging study (Figures 3 and 4), it can be noted that the range of the graphs within each sequence (over the two functional runs) is relatively stable. The shape and general trends of the EPI graphs are also consistent across the two runs; each show two local maxima located at dz values of approximately -0.5 and 0.6. One would expect from theory and previous studies that the EPI binned graph should follow approximately a $\cos^2(\theta_z)$ shape, and is therefore perfection symmetrical about dz = 0 (θ_z = 90°) [1,2]. The shape of EPI binned graph profiles was not perfectly symmetric, but does contain peaks between -1.0 and 0, and 0 and 1.0, which are nearly symmetric. It does not follow a $\cos^2(\theta_z)$ shape. The variability of the bSSFP graphs between runs is higher in terms of the number of the number and location of local maxima, but there is a consistent overall trend of decreasing between dz values of -1.0 and -0.75 and increasing between 0.75 and 1.0. The shape of the graph between layers of the same run is also highly consistent in all cases.

Conclusion

A feasible breath-hold paradigm for the measurement of large BOLD signal change at 9.4T was successfully designed and carried out with one human subject. Before imaging, a thorough behavioural study was carried out, to ensure that the paradigm could be performed with the stillness that is required to obtain high-quality fMRI measurements. Five anatomically motivated cortical layers were created within the 3D segmented gray matter, allowing for layer-specific statistics to be calculated. An analysis pipeline was created for calculating the Pearson correlation coefficient between the percent change of BOLD and orientation to the magnetic field within each of the five separate cortical layers, as well as creating binned graphs of the percent change of BOLD vs. orientation to the magnetic field. Orientation to the main magnetic field was obtained through the software MIPAV, as the magnitude component of the surface normal vector aligned with B_0 (dz). Significant ($p < 0.05$) Pearson correlation was calculated for all layers in bSSFP run 1 (ranging from 6% to 30%) and for layers 1 to 3 in run 2 (ranging for 12% to 35%). EPI run 1 resulted in significant Pearson correlation for layers 2 through 4 (ranging from -2.9% to -4.5%) and for layer 1 in run 2 (-3.5%). Binning the dz values in intervals of 0.1 and averaging ΔBOLD in each bin created layer profiles of ΔBOLD vs. dz. While none of the profiles were found to have perfect symmetry about dz = 0 ($\theta_z = 90°$), the EPI profiles did have peaks located at approximately -0.5 and 0.6 in both runs.

References

1. Gagnon L, et al. Quantifying the microvascular origin of BOLD-fMRI from first principles with two-photon microscopy and an oxygen-sensitive nanoprobe. J Neurosci., 2015:35(8):3663-3675.

2. Ogawa S and Lee TM. Magnetic Resonance Imaging of Blood Vessels at High Fields: In Vivo and in Vitro Measurements and Image Simulation. Magn. Reson. Med. 1990:16: 9-18.

3. Kim S.-G. and Bandettini P. A. Principles of BOLD Functional MRI, in Function Neuroradiology: Principles and Clinical Applications. S.H. Faro, et al., Editors. 2011, Springer: New York, Dordrecht, Heidelberg, London; 2011:293-303.

4. Lohmann G., et al. LIPSIA - a new software system for the evaluation of function magnetic resonance images of the human brain. Computerized Medical Imaging and Graphics. 2001:25(6): 449-457.

5. Handwerker DA, et al., Reducing vascular variability of fMRI data across aging populations using a breatholding task. Human Brain Mapping. 2006:28(9):846-859.

6. Thomason M and Glover G. Controlled inspiration depth reduces variance in breath-holding-induced BOLD signal. NeuroImage. 2008:39: 206-214.

7. Thomason ME et al. Breath holding reveals differences in fMRI BOLD signal in children and adults. NeuroImage. 2005:25: 824-837.